Electronic Supplementary Material (ESI) for Sustainable Energy & Fuels.

Supplementary Information

Multi-dynamic emission tailored fluoroperovskite-based down-conversion phosphors for enhancing the current density and stability of the perovskite solar cells

*Acchutharaman Kunka Ravindran [a,] *, Joel Kingston Ramesh [a], Santhosh Narendhiran [a,b], Raja Arumugam [c], Senthil Pandian Muthu [a], Ramasamy Perumalsamy [a]*

[a] Department of Physics, SSN Research Centre, Sri Sivasubramaniya Nadar College of Engineering, Chennai, Tamilnadu, 603110, India.

[b] Department of Physics and Electronics, Christ University, Bangalore, Karanataka, 560029, India.

[c] CNR-SPIN, c/o University of Salerno, Fisciano, 84084, Salerno, Italy.

*Corresponding Author: Acchutharaman Kunka Ravindran

Email: acchuthan2017@gmail.com

Tel: +91 8610944135

Address: Department of Physics, SSN Research Centre, Sri Sivasubramaniya Nadar College of Engineering, Chennai-603110, Tamilnadu, India.

1. Pre-preparations for device fabrication

Etching and cleaning of FTO substrates: FTO substrates (surface resistivity of ~8 Ω/sq) were patterned with the help of zinc dust and diluted HCl, in order to protect the device from the shunting issue. The patterned FTO substrates were washed with deionized water, acetone and IPA, each for 15 min in an ultrasonic bath. Finally, the substrates were subjected to UV-ozone cleaning for 10 min in order to remove the organic contaminations.

Compact TiO_2 (c-TiO_2) precursor solution: c-TiO_2 precursor solution was prepared by dissolving 0.3 ml of titanium diisopropoxide bis(acetylacetonate) in 5 ml of butanol.

$RbCaF_3:Eu^{3+}$ paste: The $RbCaF_3:Eu^{3+}$ paste was made by grinding the mixture of 1 g of synthesized phosphors, 0.5 g of ethyl cellulose, 4.3 ml of α-terpineol and 7.5 ml of ethanol. For the even finer paste, the obtained paste was milled in three roll-mill for 1 h.

Various wt% of $RbCaF_3:Eu^{3+}$ integrated TiO_2 colloidal solution: At first, the pristine mesoporous TiO_2 (m-TiO_2) colloidal solution was prepared by mixing TiO_2 paste with ethanol in the weight ratio of 2:7. In a similar way, the DC phosphors blended TiO_2 colloidal solution was prepared by adding $RbCaF_3:Eu^{3+}$ paste with TiO_2 paste in the weight ratios of 5:95, 10:90 and 15:85.

Perovskite precursor solution: $MAPbI_3$ is a commonly used organo-metal halide perovskite absorber for PSC. Although several researchers have shown that the addition of certain cations or halides into this $MAPbI_3$ has improved the device performance, in this study we used the $MAPbI_3$ without any modifications to explore the precise impact of down-conversion phosphors on the performance of PSCs. For that, its precursor materials PbI_2 and MAI are taken at an equimolar ratio of 1.2 M and dissolved in a mixed solvent of 0.75 ml of DMF and 0.25 ml of DMSO. Further, the precursor solution is stirred overnight at 60 °C.

2. Diffused reflectance study of $RbCaF_3:Eu^{3+}$

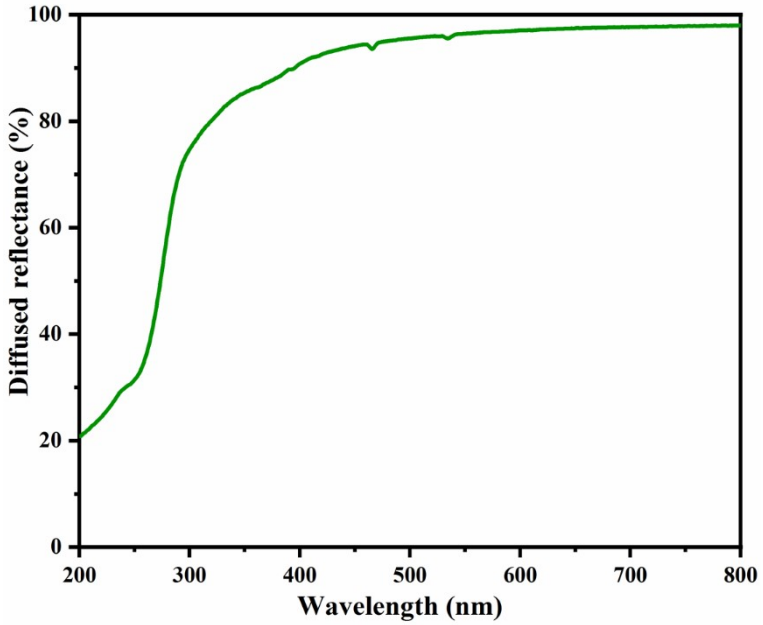

Figure S1 Diffused reflectance spectrum of $RbCaF_3:Eu^{3+}$.

3. Schematic diagram for the plausible diffusion, scattering and trapping of light due to the combination of different sizes of cubic or multi-facetted DC phosphors

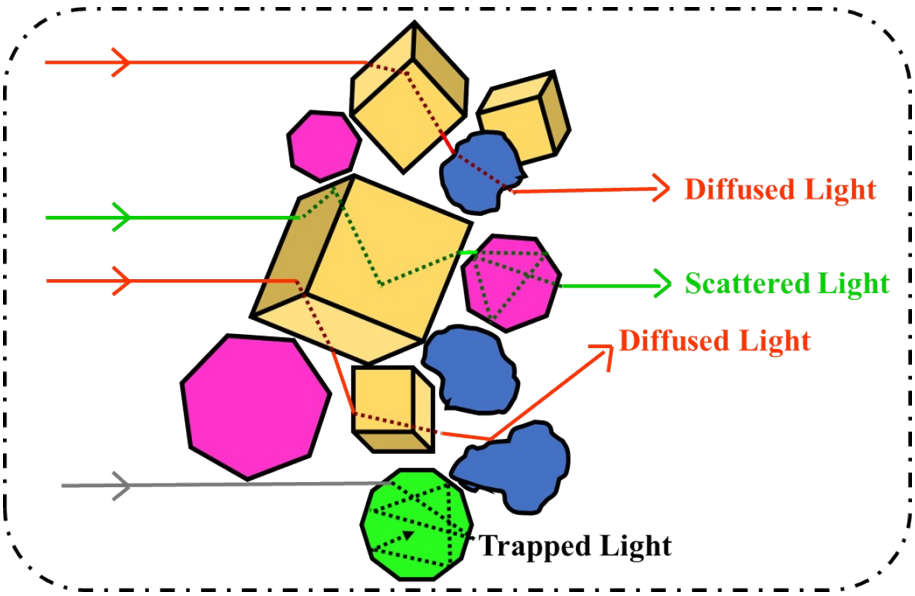

Figure S2 Plausible diffusion, scattering and trapping of light due to the combination of different sizes of cubic or multi-facetted DC phosphors.

4. Morphological and elemental analysis of 0-DCP and 10-DCP films

To evaluate the surface of the spin-coated m-TiO_2 films, SEM image of both 0-DCP and 10-DCP films was taken and they are shown in Figure S3(a, b), respectively. Both films have greater adhesion to the FTO substrate, are transparent and do not appear to be cracked. The surface of the pristine TiO_2 film (Figure S3(a)) is found to be homogenous throughout the film with no impurity or defect in it.

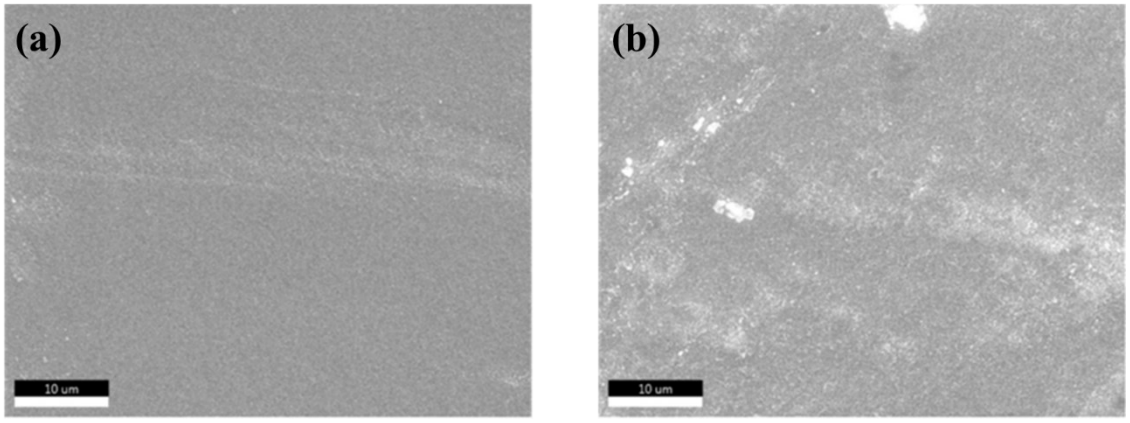

Figure S3 SEM image of (a) 0-DCP and (b) 10-DCP.

On the other hand, the distribution of fluoro-phosphors is confirmed in the 10-DCP sample through a bright luminescence. The slightly rough surface with distributed luminescent granular-like crystallization was spotted on the surface of the sample 10-DCP (Figure S3(b)). We infer that such distinguishable granular-like crystallization is due to the aggregated and micro-sized phosphors (already discussed in the section on $RbCaF_3:Eu^{3+}$ morphological analysis), which is because of the nature of the high-temperature SSR (solid state reaction) method.

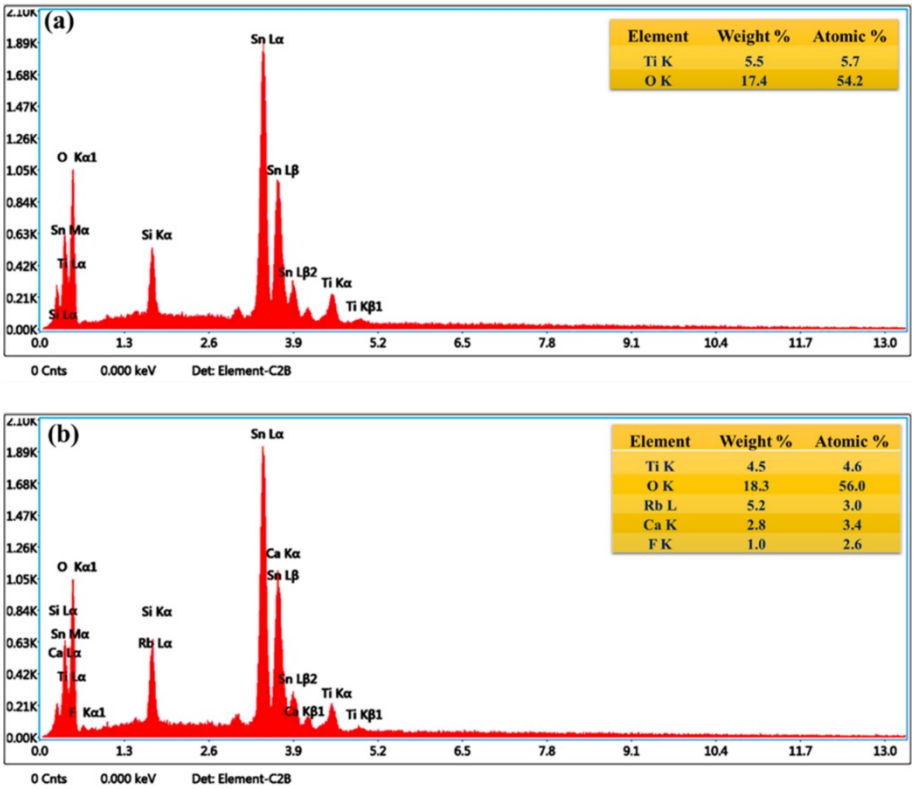

Figure S4 EDX spectra of (a) 0-DCP and (b) 10-DCP films.

The same samples were analyzed via energy dispersive X-ray (EDX) spectra as well as elemental mapping to confirm the existence of $RbCaF_3:Eu^{3+}$ in the film 10-DCP. Figure S4(a, b) shows the EDS of both 0-DCP and 10-DCP film, respectively. The sole existence of Ti and O elements in the 0-DCP film and the presence of Ti, O, Rb, Ca and F elements in the 10-DCP film are confirmed through the EDX spectra of the respective samples. Additional peaks in both the EDX spectra corresponding to Si and Sn were generated from the glass substrate and FTO layer, respectively. In the insets of the corresponding figures, the weight and atomic percentage of the elements found using EDS spectra are tabulated.

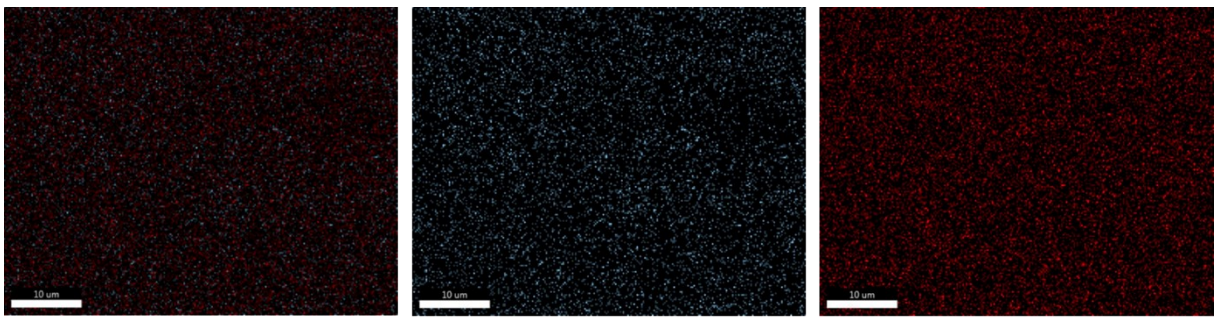

Figure S5 Elemental mapping images of sample 0-DCP.

The elemental mapping images of the same 0-DCP and 10-DCP films are shown in Figures S5 and S6, respectively. As it can be seen from Figure S5, the 0-DCP film has the elements Ti and O spread quite homogeneously. Similarly, the homogeneous distribution of materials related to the fluoroperovskite phosphors (Rb, Ca and F) with TiO_2 (Ti and O) in the sample 10-DCP is evident in Figure S6. Also, it is noted that there is no evidence for the presence of impurities except the above-mentioned elements.

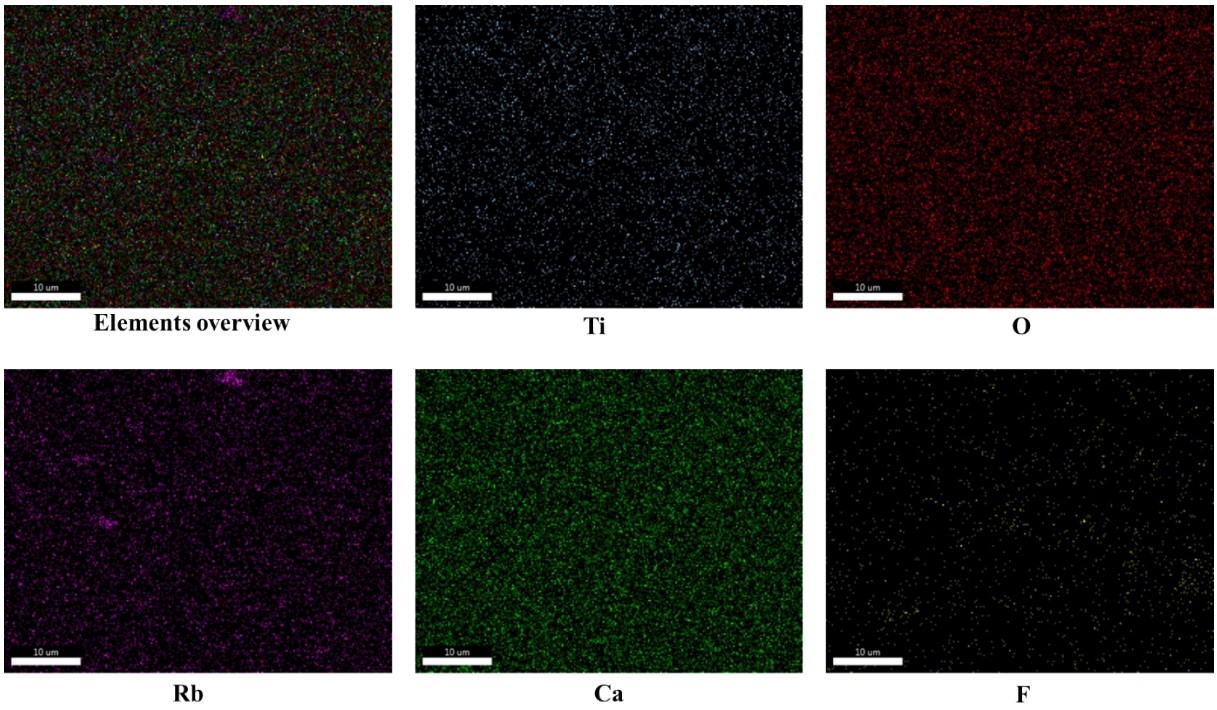

Figure S6 Elemental mapping images of 10-DCP.

5. UV-Vis transmittance study for the ETLs based on 0, 5, 10 and 15-DCP

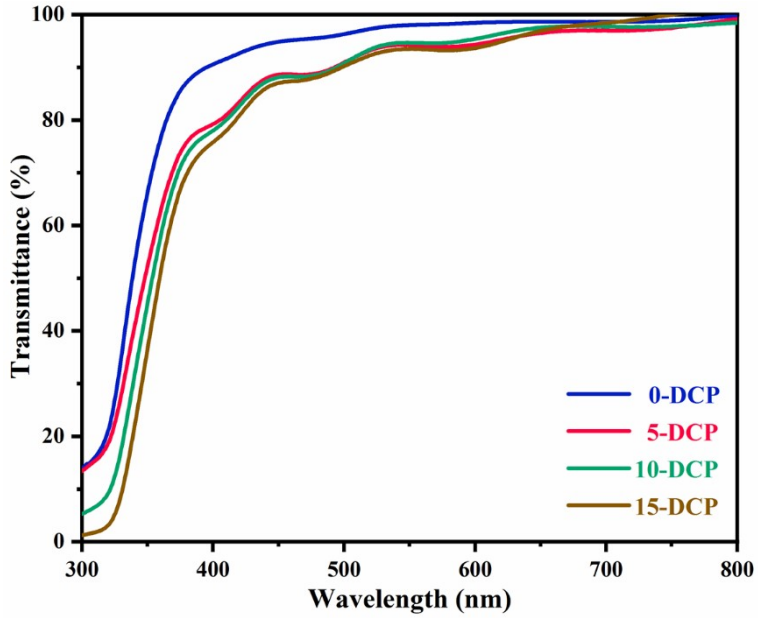

Figure S7 UV-Vis transmittance spectrum of 0, 5, 10 and 15-DCP-based ETLs.

6. FESEM image of perovskite film:

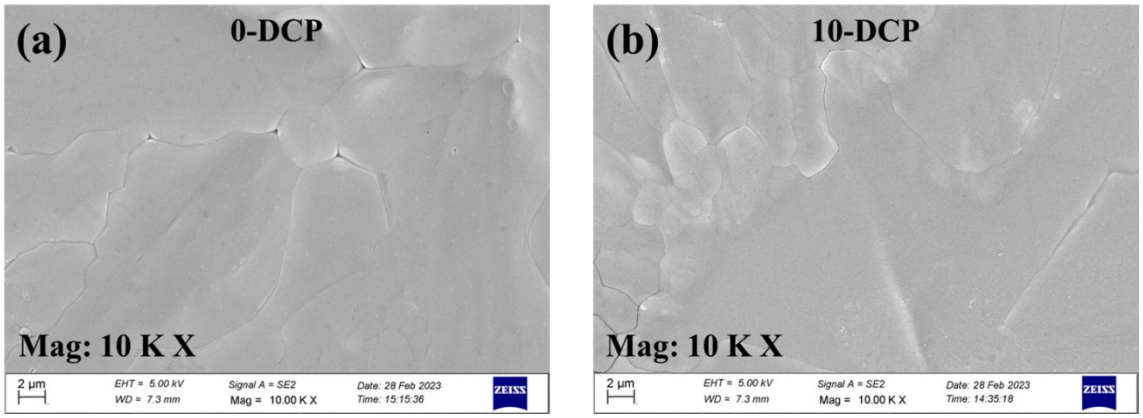

Figure S8 FESEM images of perovskite film deposited over 0 and 10 DCP-based ETL

7. Experimental setup for UV-stability analysis

Figure S9 Digital image of the experimental setup of UV irradiation on the perovskite layer.